Inhibition of FBP1 expression by KMT5A through TWIST1 methylation is one of the mechanisms leading to chemoresistance in breast cancer

XUE PENG*, LISI MA*, XUAN CHEN*, FEN TANG and XIANGYUN ZONG

Department of Breast Surgery, Shanghai Sixth People's Hospital Affiliated to Shanghai Jiao Tong University School of Medicine, Shanghai 200233, P.R. China

Received March 4, 2024; Accepted May 31, 2024

DOI: 10.3892/or.2024.8769

Abstract. Lysine methyltransferase 5A (KMT5A) is the sole mammalian enzyme known to catalyse the mono-methylation of histone H4 lysine 20 and non-histone proteins such as p53, which are involved in the occurrence and progression of numerous cancers. The present study aimed to determine the function of KMT5A in inducing docetaxel (DTX) resistance in patients with breast carcinoma by evaluating glucose metabolism and the underlying mechanism involved. The upregulation or downregulation of KMT5A-related proteins was examined after KMT5A knockdown in breast cancer (BRCA) cells by Tandem Mass Tag proteomics. Through differential protein expression and pathway enrichment analysis, the upregulated key gluconeogenic enzyme fructose-1,6-bisphosphatase 1 (FBP1) was discovered. Loss of FBP1 expression is closely related to the development and prognosis of cancers. A dual-luciferase reporter gene assay confirmed that KMT5A inhibited the expression of FBP1 and that overexpression of FBP1 could enhance the chemotherapeutic sensitivity to DTX through the suppression of KMT5A expression. The KMT5A inhibitor UNC0379 was used to verify that DTX resistance induced by KMT5A through the inhibition of FBP1 depended on the methylase activity of KMT5A. According to previous literature and interaction network structure, it was revealed that KMT5A acts on the transcription factor twist family BHLH transcription factor 1 (TWIST1). Then, it was verified that TWSIT1 promoted the expression of FBP1 by using a dual-luciferase reporter gene experiment. KMT5A induces chemotherapy resistance in BRCA cells by promoting cell proliferation and glycolysis. After the knockdown of the KMT5A gene, the FBP1 related to glucose metabolism in BRCA was upregulated. KMT5A knockdown expression and FBP1 overexpression synergistically inhibit cell proliferation and block cells in the G2/M phase. KMT5A inhibits the expression of FBP1 by methylating TWIST1 and weakening its promotion of FBP1 transcription. In conclusion, KMT5A was shown to affect chemotherapy resistance by regulating the cell cycle and positively regulate glycolysis-mediated chemotherapy resistance by inhibiting the transcription of FBP1 in collaboration with TWIST1. KMT5A may be a potential therapeutic target for chemotherapy resistance in BRCA.

Correspondence to: Dr Xiangyun Zong, Department of Breast Surgery, Shanghai Sixth People's Hospital Affiliated to Shanghai Jiao Tong University School of Medicine, 600 Yishan Road, Shanghai 200233, P.R. China
E-mail: tigerzong@msn.com

*Contributed equally

Abbreviations: BRCA, breast cancer; DTX, docetaxel; FBP1, fructose-1,6-bisphosphatase; IC50, half maximal inhibitory concentration; KMT5A, lysine methyltransferase 5A; RT-qPCR, reverse transcription-quantitative polymerase chain reaction

Key words: KMT5A, glucose metabolism, chemoresistance, BRCA, FBP1

Introduction

Chemotherapy, as a comprehensive treatment for breast cancer (BRCA), has improved the survival rate of patients with BRCA, to a certain extent (1). Docetaxel (DTX), a semisynthetic derivative of paclitaxel, is a second-generation paclitaxel anticancer drug and serves as the cornerstone of various BRCA chemotherapy regimens (2). However, the occurrence of drug resistance has limited the clinical efficacy of taxanes to some extent (3). Congenital and acquired chemoresistance constitute important reasons for long-term treatment failure in patients with BRCA (4). The mechanisms of congenital resistance mainly include decreased drug activation, abnormal expression of membrane transporters such as ABC transporters (5), abnormal apoptosis or autophagy-induced chemotherapy resistance (6), changes in the expression and/or function of drug targets, reduced efficiency of drug-target interactions (7), and enhanced DNA damage repair ability (8). Acquired resistance is influenced by genetic or environmental factors that promote the development of resistant stem cells or induce mutations in enzymes involved in related metabolic pathways (9). Currently, an increasing number of studies have focused on the role of metabolic reprogramming in tumor chemotherapy resistance (10).

Lysine methyltransferase 5A (KMT5A, also known as SETD8; SET8; SET07; PR-Set7, and PR/SET07) is a member of the SET domain-containing methyltransferase family that specifically catalyses the addition of histone H4 lysine 20 (H4K20) me1 (11). The expression of this protein methyltransferase fluctuates during the cell cycle and peaks during the G2/M transition (12). KMT5A affects the development and progression of a variety of cancers (13-15) and causes a variety of tumors to develop chemotherapy resistance (16). Fructose-1,6-bisphosphatase 1 (FBP1) acts as a key enzyme for gluconeogenesis and regulates energy metabolism in tumor cells, and it is downregulated in a variety of cancers, which affects the evolution of drug resistance and the prognosis of cancers (17-19). KMT5A participates in regulating the energy metabolism process of malignant tumors and promotes tumor cell invasion and metastasis (20). In the present study, the expression of KMT5A and FBP1 in normal BRCA and paraneoplastic tissues were analysed. Changes in DTX sensitivity in stable KMT5A-knockdown BRCA cells were detected with a Cell Counting Kit-8 (CCK-8) kit. The mechanism through which KMT5A promotes DTX resistance in BRCA was preliminarily explored by inhibiting FBP1 to provide a theoretical basis for overcoming drug resistance.

Materials and methods

Cell lines and cell culture. The MCF-7 cell line was purchased from the Chinese Academy of Sciences (Shanghai, China), the MDA-MB-231 cell line was donated by Fudan University Cancer Hospital (Shanghai, China), and the 293T cell line was purchased by Shanghai Sixth Hospital Central Laboratory (Shanghai, China). The MCF-7 and 293T cell lines were cultured in DMEM supplemented with 10% fetal bovine serum (FBS) (Wuhan Servicebio Technology Co., Ltd.) at 37˚C and 5% CO_2. MDA-MB-231 cell line was cultured in Leibovitz's L-15 medium supplemented with 10% FBS without CO_2 at 37˚C. The cells were digested with 0.25% trypsin-EDTA (cat. no. 25200072) (Gibco; Thermo Fisher Scientific, Inc.) and passaged.

Plasmids. The full-length cDNAs of KMT5A and FBP1 were obtained by PCR amplification from human tissue and directly connected downstream of the CMV promoter of the lentiviral expression vector after enzyme digestion through ligase reaction. The overexpression plasmid was Ubi-MCS-3FLAG-SV40-EGFP-IRES-puromycin (GV358) (Shanghai GeneChem Co., Ltd.), and GV358-Control and GV358-KMT5A (Shanghai GeneChem Co., Ltd.) were constructed by sequencing and identification. The vector with the correct expression sequence of the recombinant FBP1 gene was selected by gene sequencing, and the plasmid GV358-Control and GV358-FBP1 (Shanghai GeneChem Co., Ltd.) were constructed by sequencing. shRNA targets design software (https://rnaidesigner.thermofisher.com/rnaiexpress/sort.do) from human KMT5A (NM_020382) was used. The synthetical oligos were inserted into the lentivirus expression plasmid hU6-MCS-Ubiquitin-EGFP-IRES-puromycin (GV248) (Shanghai GeneChem Co., Ltd.) (additional vector information and the sequences of shRNA are included in Tables SI and SII). Empty vectors were used as negative controls in the aforementioned plasmid construction experiments of overexpression and knockdown expression.

Lentivirus production and transduction. For virus packaging, 293T cells were seeded into a 10-cm culture dish with puromycin (2 μg/ml). When the cells reached a density of 60-70%, KMT5A(GV358-KMT5A) (2.67 μg)/shKMT5A(GV248-KMT5A) (4 μg)/FBP1(GV358-FBP1) (1.33 μg) plasmid or control vector was transfected into 293T cells along with lentiviral helper plasmid (ps-PAX2, pMD2G tagged in green fluorescent protein) (Shanghai GeneChem Co., Ltd.) using Lipofectamine® 3000 transfection kit (Invitrogen; Thermo Fisher Scientific, Inc.) at 25˚C. The proportions were as follows: target plasmid: ps-PAX2: pMD2G=1:3:4. After transfection for 48 h, the culture media containing recombinant lentivirus were collected, filtered, concentrated, purified and stored at -80˚C. The sequence of shRNA was CGCAACAGA ATCGCAAACTTA.

Lentiviral infection of human BRCA cells. The MDA-MB-231 cells and MCF-7 cells were cultured in 6-well plates. Then prepared recombinant lentivirus was added into the culture medium with multiplicity of infection of 20. After 72 h infection, the GFP expression was observed under a fluorescence microscope to evaluate lentivirus infection efficiency. Total RNA and protein were extracted 72 h after infection.

Reverse transcription-quantitative (RT-q) PCR. The cells were collected (6-well plate with 80% cell density) and centrifuged at 14,000 x g for 5 min at 25˚C, after which total RNA was extracted with TRIzol® reagent (Shanghai Pufei Biotechnology Co., Ltd.). Total RNA (2.0 μg) was used for complementary DNA (cDNA) synthesis via a Promega M-MLV kit (cat no. M1701; Promega Corporation) following the manufacturer's protocol. RT-qPCR was conducted with SYBR Premix Ex Taq (Takara Bio, Inc.) via a two-step method, and a melting curve was prepared for quantitative data analysis. The thermocycling conditions were as follows: 95˚C for 10 min, 95˚C for 15 sec, 59˚C for 40 sec, 72˚C for 45 sec, and the cycles were 40 times. The relative mRNA levels were calculated using the comparative Ct method ($2^{-\Delta\Delta Cq}$) (21). The primer pairs were designed with Primer Express 3.0 (ABI Inc.). The sequences of primers (Biosune; http://www.biosune.com/) were as follows: KMT5A forward, 5'-GAAGTCCGAGGAACAGAAG-3' and reverse, 5'-ACAGGGTAGAAATCCGTAA-3'; FBP1 forward, 5'-TCTACCAACGTGACAGGTGA-3' and reverse, 5'-ATC AAGGGGATCAAAACAGA-3'; and β-actin forward, 5'-GCG TGACATTAAGGAGAAGC-3' and reverse, 5'-CCACGTCAC ACTTCATGATGG-3'.

In vitro chemosensitivity assay. The MTT assay was used to evaluate the cytotoxicity of DTX against BRCA cells. First, the MDA-MB-231 cells were incubated at 37˚C after seeding into 96-well plates at $5x10^4$ cells/well for 24 h. Then, the cells were treated with gradient concentrations of DTX at equal concentrations. MTT solution (20 μl, 5 mg/ml) (Shanghai Dingguo Biotechnology Co., Ltd.) was added to each well according to the design time. After 4 h of incubation at 37˚C, the culture medium containing unreacted MTT was completely removed from the wells, and dimethyl sulfoxide (100 μl) was added to

each well. After the samples were oscillated for 3-5 min, the OD values were detected by a microplate reader at 490/570 nm. Finally, the data were analyzed.

Detection of drug sensitivity by Cell Counting Kit-8 (CCK-8). Cell proliferation and cell activities were measured by a CCK-8 assay (Dojindo Laboratories, Inc.). All the MDA-MB-231 or MCF-7 cells were plated at $1x10^4$ cells per well and treated with different concentrations of DTX for 48 h. Then, CCK-8 solution (100 μl/well) was added to all the wells and incubated at 37˚C for 4 h, the absorbance was read at 450 nm, and calculated the percentage of cell viability.

BRCA cell lines were treated with KMT5A inhibitor UNC0379 (0, 5 or 10 μM) (MedChemExpress) and DTX (20 μM) for 48 h. A total of 10 μl of diluted CCK-8 was added into each well and cells were incubated in a 5% CO_2 incubator for 2 h at 37˚C. Absorbance was measured at 450 nm.

Flow cytometry. When the cells cultured in 6-cm dishes reached to a confluence rate of ~80% (the cells did not reach the growth plateau stage), they were digested with pancreatic enzymes and collected, and three wells were set in each group (to ensure a sufficient number of cells on the machine, $\geq 10^6$ cells were used). The cells were centrifuged at 350 x g for 5 min at 4˚C, washed with precooled Dulbecco's phosphate-buffered saline (DPBS) (pH=7.2~7.4) at 4˚C and precipitated once. The cells were centrifuged at 350 x g for 5 min at 4˚C. The cell staining agent used was 40X propidium iodide (PI) (2 mg/ml) (MilliporeSigma), 100X RNase (10 mg/ml) (Thermo Fisher Scientific, Inc.), 1X DPBS and 25X Triton X-100 (MilliporeSigma) (25:10:1,000:40). The cell suspension was added to a certain volume of cell staining solution (0.6-1 ml) to ensure that the cell passage rate was 300 to 800 cells/sec. After machine (CytoFLEX; Beckman Coulter, Inc.) detection, the data analysis was performed by ModFit software (5.0) (Verity Software House, Inc.).

Immunohistochemistry (IHC). A total of 60 patients (age range, 31-82 years) with BRCA admitted to Shanghai Sixth People's Hospital Affiliated to Shanghai Jiao Tong University School of Medicine from August 2023 to December 2023 were selected as the present study's subjects. The present study was approved (approval no. YS-2017-006) by the Ethics Committee of the Sixth People's Hospital Affiliated to Shanghai Jiao Tong University School of Medicine (Shanghai, China), and written informed consent was obtained from each patient. The inclusion criteria were as follows: i) Meeting the diagnostic criteria for BRCA; ii) Surgical resection was performed, and samples of BRCA tissues and adjacent tissues were obtained. The diagnosis of BRCA was confirmed by pathological examination, iii) for the first time, no anticancer treatment such as endocrine therapy, radiotherapy and chemotherapy was taken before surgery, iv) women, v) complete clinical data; and vi) signed informed consent for the present study. Exclusion criteria were the following: i) Combined with systemic infectious diseases, cardiovascular and cerebrovascular diseases, liver and kidney insufficiency; ii) combined with other types of tumors; iii) combined with terminal disease; iv) tissue samples that cannot be obtained; and v) ment0al system diseases and suicidal tendencies.

Normal tumor and breast tissues were excised from patients. These tissues were fixed in 10% neutral buffered formalin, embedded in paraffin at 4˚C for 12 h, sectioned (5 μm), and stained with haematoxylin-eosin staining. Immunohistochemical staining using KMT5A antibody (1:100; cat. no. PA5-102712; Thermo Fisher Scientific, Inc.; 22˚C for 1.5 h) and Rabbit IgG (H + L) cross-Adsorbed Secondary Antibody (1:2,000; cat. no. A-11008; Thermo Fisher Scientific, Inc.; 25˚C for 30 min) was performed by the Department of Pathology at Shanghai Sixth People's Hospital Affiliated with Shanghai Jiao Tong University School of Medicine. KMT5A immunohistochemical markers were assessed using light microscopy. The immunostained slides were scored according to the proportion of tumor cells that exhibited nuclear staining. KMT5A expression was considered positive when >25% of the tumor cell nuclei were stained (Table SIII).

Western blotting. MCF-7 or MDA-MB-231 cells in 6-well plates were collected and washed twice with phosphate-buffered saline (PBS) (Wuhan Servicebio Technology Co., Ltd.). Protein was extracted from MCF-7 or MDA-MB-231 cells by RIPA lysis buffer (Beyotime Institute of Biotechnology). The concentration of the proteins was determined with a BCA protein assay kit (Beyotime Institute of Biotechnology). The protein lysates were separated by sodium dodecyl sulphate-polyacrylamide gel electrophoresis. The separation gel with 10% polyacrylamide was prepared, and 30 μl protein was loaded to each lane and transferred onto polyvinylidene fluoride (PVDF) membranes (MilliporeSigma). The PVDF membranes were blocked with 0.1% TBST solution (Wuhan Servicebio Technology Co., Ltd.) containing 5% skim milk at 25˚C for 1 h. After the membranes were incubated with primary antibodies KMT5A, (1:1,000; cat. no. 14063-1-AP; Proteintech Group, Inc.; 37˚C for 1 h;) and FBP1 (1:2,000; cat. no. 12842-1-AP; Proteintech Group, Inc.; 25˚C for 1.5 h;) and secondary antibody Multi-rAb HRP-Goat Anti-Rabbit Recombinant Secondary Antibody (1:5,000; cat. no. RGAR001; Proteintech Group, Inc.; 25˚C for 1 h;), an enhanced chemiluminescence (ECL) kit (Thermo Fisher Scientific, Inc.) and X-ray (Carestream Health, Inc.) were used to visualize the membranes. The X-rays were removed, the samples were allowed to dry, and the blots were analysed. Because the molecular weights of KMT5A and actin were both 43 KD. At first, the target protein KMT5A was incubated. After KMT5A was stripped, the internal reference protein actin was incubated on the same membrane.

Dual-luciferase reporter assay. KMT5A 3'-UTR sequence was obtained from KMT5A and twist family BHLH transcription factor 1 (TWIST1) full-length cDNA vector (Shanghai GeneChem Co., Ltd.) and sub-cloned to pcDNA3.1-control vector (Shanghai GeneChem Co., Ltd.) as wild-type vector pcDNA3.1-KMT5A-3'-UTR-WT (KMT5A-WT) and pcDNA3.1-TWIST1-3'-UTR respectively. The mutant vector pcDNA3.1-KMT5A-3'-UTR-Mut (KMT5A-R295G) was obtained by site-directed mutagenesis using QuikChange® Site-Directed Mutagenesis Kit (Stratagene; Agilent). MDA-MB-231 cells were seeded in a 24-well culture plate in triplicate and were transfected followed by pcDNA3.1-KMT5A-3'-UTR-WT or

pcDNA3.1-KMT5A-3'-UTR-MutorpcDNA3.1-TWIST1-3'-UTR by ExFect Transfection Reagent (Vazyme Biotech Co., Ltd.) according to the manufacturer's procedure.

Cells were seeded in 24-well plates at a density of 500 μl/well and transfected with the target plasmid (Table SIV). After 48 h at 37˚C, the luciferase activity of each group was detected by a dual luciferase system (cat. no. E1910; Promega Corporation). The cell lysate was supplemented with firefly luciferase (100 μl), after which firefly luciferase activity was measured (F value). After adding *Renilla* luciferase (100 μl), the cell lysate was immediately placed into the fluorescence detector to calculate the *Renilla* luciferase activity (R-value). Based on the F and R values of each group detected previously, the relative luciferase activity was calculated to get promoter activity. The primers for the FBP1 promoter were: forward, 5'-GACAGAAGGGCCAGGTGA-3' and reverse, 5'-GCC AGAGAGAAAGCTATGACTG-3'; transcription start site: (967-979 bp) AAGCCAGATGA.

Determination of glucose uptake and lactate production. To detect glucose consumption and lactate production in BRCA cells, a Glucose Uptake Colorimetric Assay Kit (cat. no. K676-100; BioVision, Inc.; Abcam) and a Colorimetric/Fluorometric Assay Kit (cat. no. K607-100; BioVision, Inc.; Abcam) were used according to the manufacturer's instructions. A total of 2,000 MDA-MB-231 cells were seeded in each well of a 96-well plate and incubated for 48 h at 37˚C. After that, based on the Glucose Uptake Colorimetric Assay Kit protocol, absorbance was measured at 412 nm in a microplate reader at 37˚C every 5 min until the 100 pmol standard reached 1.5-2.0 OD. An endpoint reading of all samples and standards was taken. The 2-deoxy-D-glucose 6P standard curve was plotted and the glucose intake was calculated. Based on the Colorimetric/Fluorometric Assay Kit protocol, absorbance was measured at 570 nm in a microplate reader. The lactate standard curve was plotted and sample lactate concentration was calculated. The glucose and lactate levels were calculated using a standard calibration curve prepared under the same conditions.

TMT labelling and bioinformatics analysis. The peptide mixture (100 μg) of each sample was labelled by TMT reagent according to the manufacturer's instructions (Thermo Fisher Scientific, Inc.). TMT-labelled peptides (10 μl) were fractionated by peptide fractionation with reversed phase chromatography using the Agilent 1260 infinity II HPLC. Each fraction was injected for nano LC-MS/MS analysis. The peptide mixture was loaded onto the C18-reversed phase analytical column (Thermo Fisher Scientific, Inc.; Acclaim PepMap RSLC 50 μm x15 cm, nano viper, P/N164943) in buffer A (0.1% formic acid) and separated with a linear gradient of buffer B (80% acetonitrile and 0.1% formic acid) at a flow rate of 300 nl/min. LC-MS/MS analysis was performed on a Q Exactive Plus mass spectrometer (Thermo Fisher Scientific, Inc.) that was coupled to Easy nLC (Thermo Fisher Scientific, Inc.) for 60 min. MS/MS raw files were processed using MASCOT engine (version 2.6; Matrix Science, Ltd.) embedded into Proteome Discoverer 2.2, and searched against the UniProt database, downloaded from https://www.uniprot.org/, including HomoSapiens_20367_20200226 sequences. Proteins with Fold change >1.2 and adjusted. P<0.05 (Student's t-test) were considered to be differentially expressed proteins. The annotation from gene ontology (GO) terms to proteins was completed by Blast2GO Command Line. After the elementary annotation, InterProScan (https://www.ebi.ac.uk/interpro/) was used to search the EBI database (https://www.ebi.ac.uk/) by motif and then add the functional information of motif to proteins to improve annotation. Then further improvement of annotation and connection between GO terms were carried out (Table SV). Fisher's Exact Test was used to enrich GO terms by comparing the number of differentially expressed proteins and total proteins associated to GO terms. Pathway analysis was performed using Kyoto Encyclopedia of Genes and Genomes (KEGG) database (https://www.genome.jp/kegg/pathway.html). Fisher's Exact Test was used to identify the significantly enriched pathways by comparing the number of differentially expressed proteins and total proteins associated to pathways (Tables SVI-SX) and protein structure (Table SXI).

Source databases. The partial immunohistochemistry images and interaction network were obtained from The Human Protein Atlas (HPA, https://www.proteinatlas.org/) (22). The gene expression levels in healthy breast and BRCA were obtained from The University of Alabama at Birmingham database (UALCAN, https://ualcan.path.uab.edu/index.html) (23). Some data were downloaded from the TCGA database (https://www.cancer.gov/ccg/research/genome-sequencing/tcga). The expression data of KMT5A gene in MDA-MB-231 and MCF-7 cell lines was downloaded from the 'Expression 23Q4 Public' dataset of the Cancer Cell Line Encyclopedia database (CCLE, https://www.broadinstitute.org/ccle) (24).

Ethics. The present study was approved (approval no. YS-2017-006) by the Ethics Committee of the Sixth People's Hospital Affiliated to Shanghai Jiao Tong University School of Medicine (Shanghai, China), and written informed consent was obtained from each patient.

Statistical analysis. SPSS software 26.0 (IBM Corp.) was used for Pearson correlation statistical analyses. Most of the data were analyzed and bar charts were generated with GraphPad Prism 9.5 software (Dotmatics). Volcano map was expressed by R studio (4.3.2) (RStudio, Inc.). KEGG and GO analysis were drawn by bioinformatics (https://www.bioinformatics.com.cn). Data are presented as the mean ± standard deviation (minimum three repeats, depending of the experiments). Comparisons between groups were analyzed using one-way ANOVA followed by Bonferroni's (for comparing within treatment conditions) or Dunnett's (for comparing between treatment conditions) or Multiple Comparison Test. P<0.05 was considered to indicate a statistically significant deference.

Results

KMT5A is upregulated in BRCA tissues. The UALCAN database was searched (https://ualcan.path.uab.edu/index.html) (23) to determine the expression of KMT5A in BRCA. KMT5A was upregulated in BRCA (P<0.05). The expression level of KMT5A was the highest in triple-negative BRCA (P<0.05) and the lowest in the luminal subtype (P<0.05) (Fig. 1A) (All data

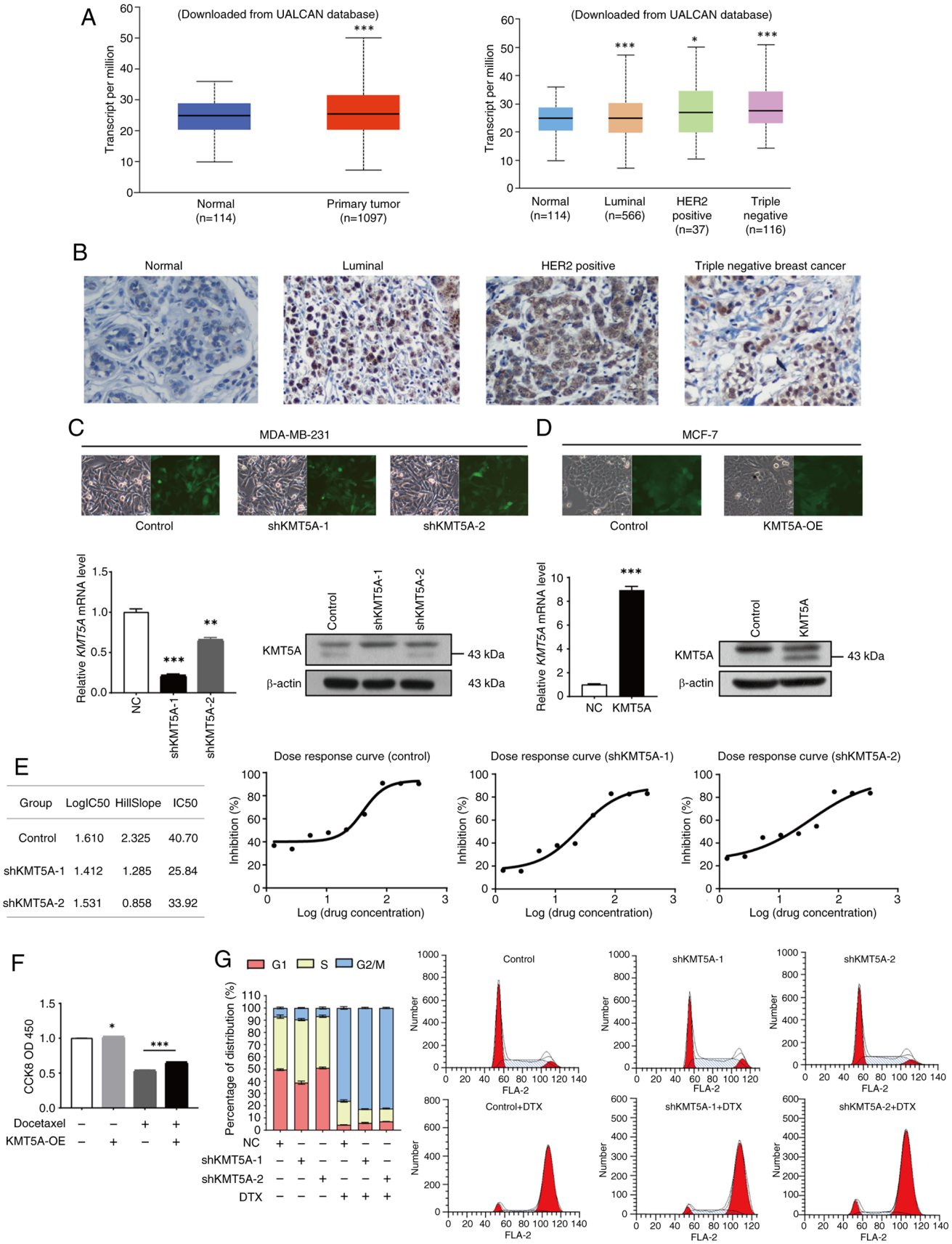

Figure 1. KMT5A mediates DTX resistance in BRCA cells. (A) Expression of KMT5A in BRCA. (B) Representative images of immunohistochemical staining of KMT5A in BRCA tumors. (C and D) After 72-h infection, cells were observed, and images were captured by fluorescence microscope. Magnification, x100. Expression of KMT5A in BRCA cells was detected by reverse transcription-quantitative PCR and western blotting. (E) MTT assay was performed to examine the cell viability and proliferation. (F) The sensitivity of MCF-7 cell line overexpressing KMT5A to DTX was detected by a CCK-8 assay. (G) Effect of KMT5A knockdown and/or DTX on the cell cycle of the MDA-MB-231 cell line. *P<0.05; **P<0.01 and ***P<0.001. KMT5A, lysine methyltransferase 5A; DTX, docetaxel; BRCA, breast cancer; CCK-8, Cell Counting Kit-8; UALCAN, the university of Alabama at Birmingham database; sh, short hairpin; OE, overexpression; NC, negative control.

and significance levels were from the UALCAN database). The immunohistochemical results of 60 patients were included in the analysis. Patients ranged in age from 31 to 82 years, with a median age of 60 years. IHC also revealed that KMT5A was highly expressed in BRCA tissues (Fig. 1A).

Knockdown of KMT5A in MDA-MB-231 cells and overexpression of KMT5A in MCF-7 cells. The expression of endogenous KMT5A was lower in MCF-7 cell lines (5.35), however higher in MDA-MB-231 cell lines (5.74) (Data was from 'Expression 23Q4 Public' dataset of the CCLE database). Therefore, lentivirus-mediated KMT5A shRNA silenced KMT5A expression in MDA-MB-231 cell line, and overexpressed KMT5A mRNA in MCF-7 cell line. As demonstrated in Fig. 1B, the stably transfected MDA-MB-231 BRCA cell line was subsequently generated via lentivirus infection and puromycin resistance screening and subsequently divided into three groups for identification. The negative control (NC) group was generated by stably transforming MDA-MB-231 cells with a control lentiviral vector. The shKMT5A-1 and shKMT5A-2 group were stably transformed into MDA-MB-231 cells via the LVpFU-GW-007-mediated transfer of the lentiviral vector. KMT5A knockdown was confirmed at the mRNA and protein levels. The shKMT5A-1 and shKMT5A-2 groups exhibited significantly lower levels of the KMT5A mRNA and protein ($P<0.05$) (Fig. 1C). Furthermore, the knockdown efficiency of shKMT5A-1 was greater than that of shKMT5A-2. Moreover, RT-qPCR and western blot analysis confirmed that KMT5A was significantly highly expressed in MCF-7 cells transfected with an overexpression lentiviral vector (Fig. 1D).

Effect of KMT5A on sensitivity to chemical resistance and the cell cycle. To further confirm whether KMT5A knockdown affects chemical resistance and the cell cycle, MDA-MB-231 cells were treated with DTX, the half-maximal inhibitory concentration (IC_{50}) was measured, dose-response curves were constructed for each group, and the proportions of cells in different phases were evaluated. After KMT5A knockdown, the IC_{50} of DTX decreased significantly (Fig. 1E). In the DTX positive KMT5A-OE negative group, the proliferation rate of MCF-7 cells when DTX (20 μM) was added only was 53.9%. However, in the case of high expression of KMT5A, the cell activity increased to 66.5% after DTX addition compared with the DTX positive KMT5A-OE negative group. It was revealed that high expression of KMT5A antagonized DTX and promoted cell proliferation (Fig. 1F). KMT5A expression may mediate the development of DTX resistance in BRCA cells.

In the control group, the proportion of G1-phase cells was 49.51±0.71%, the proportion of S-phase cells was 43.43±1.38%, and the proportion of G2/M-phase cells was 7.06±0.67%. The proportions of G1 phase cells, S phase cells, and G2/M phase cells in the shKMT5A-1 group were 38.91±1.27, 51.60±0.93% and 9.49±0.37%, respectively. After adding DTX, the proportion of cells in the G2/M phase increased, and the proportion of cells in the S phase decreased significantly. In the control group, the proportion of G2/M phase cells increased to 82.82±0.53%, and the proportion of S phase cells decreased to 11.28±0.36%. The proportion of G2/M phase cells in the shKMT5A-1 group was 76.15±1.04%, and the proportion of S phase cells was 19.50±0.96%. After KMT5A knockdown, the proportion of S-phase cells was markedly greater than that of parental cells (Fig. 1G). First of all, DTX is effective against various pathological types of BRCA, including triple-negative BRCA, and remains the first-choice chemotherapy drug for this type. The triple-negative BRCA cell line (MDA-MB-231) is less sensitive to DTX than the hormone receptor-positive MCF-7 cell line. Secondly, the mechanism of DTX is to enhance the polymerization of tubulin and inhibit the depolymerization of microtubules, leading to the formation of stable non-functional microtubule bundles, thus disrupting the mitosis of tumor cells. The present study revealed that MDA-MB-231 cell line was blocked in mitosis and remained in the G2/M phase, which is consistent with its pharmacological effect and previous findings (25).

The levels of monomethylated H4K20 and KMT5A changed dynamically during different phases of the cell cycle, and these dynamic changes regulated the progression of the cell cycle. KMT5A and monomethylated H4K20 are expressed at low levels in the S phase, and KMT5A and monomethylated H4K20 reach their peak expression in the G2/M phase. The normal process of the S phase requires KMT5A (26); therefore, after KMT5A expression was knocked down, cells were arrested in the S phase and could not enter the G2/M phase. However, DTX mainly affects M-phase cells (27); therefore, when DTX is added, the proportion of G2/M phase cells was greater than that of parent cells (negative control without DTX).

Bioinformatics analysis reveals that KMT5A knockdown induces FBP1 upregulation. To identify the downstream proteins regulated by KMT5A, protein expression levels were evaluated in the BRCA cell line MDA-MB-231 transfected with NC lentivirus (negative control) or KMT5A-targeting lentivirus (shKMT5A). A total of three samples were randomly selected from NC and shKMT5A groups, and the protein was quantitatively analyzed by TMT (Tandem Mass Tag) proteomics technology and the differentially expressed protein was screened out. The analysis of differential gene expression revealed that the expression levels of 261 proteins increased after KMT5A was knocked down. Conversely, the expression of 153 proteins was downregulated (Fig. 2A). As a key gluconeogenic enzyme, FBP1 expression increased significantly (Fold change=1.23, adjusted. $P<0.05$) after KMT5A was knocked down.

Pathway enrichment analysis demonstrated that KMT5A regulates several pathways, including the extracellular exosome and membrane pathways. In addition to these pathways being enriched, it was revealed that they were tightly connected to chemoresistance and glucose metabolism (Fig. 2B). Moreover, the 'extracellular exosome' plate differs most significantly among the cell components, and exosomes have been revealed to lead to chemical resistance in various cancers and regulate chemical resistance in several ways (Fig. 2C). Exosomes transport glycolytic enzymes. According to the proteomic analysis results, exosomes lead to metabolic reprogramming and promote alterations in both glucose metabolism and lactate production.

Overexpressed FBP1 in MDA-MB-231 cells. UALCAN database was searched and was revealed that the expression

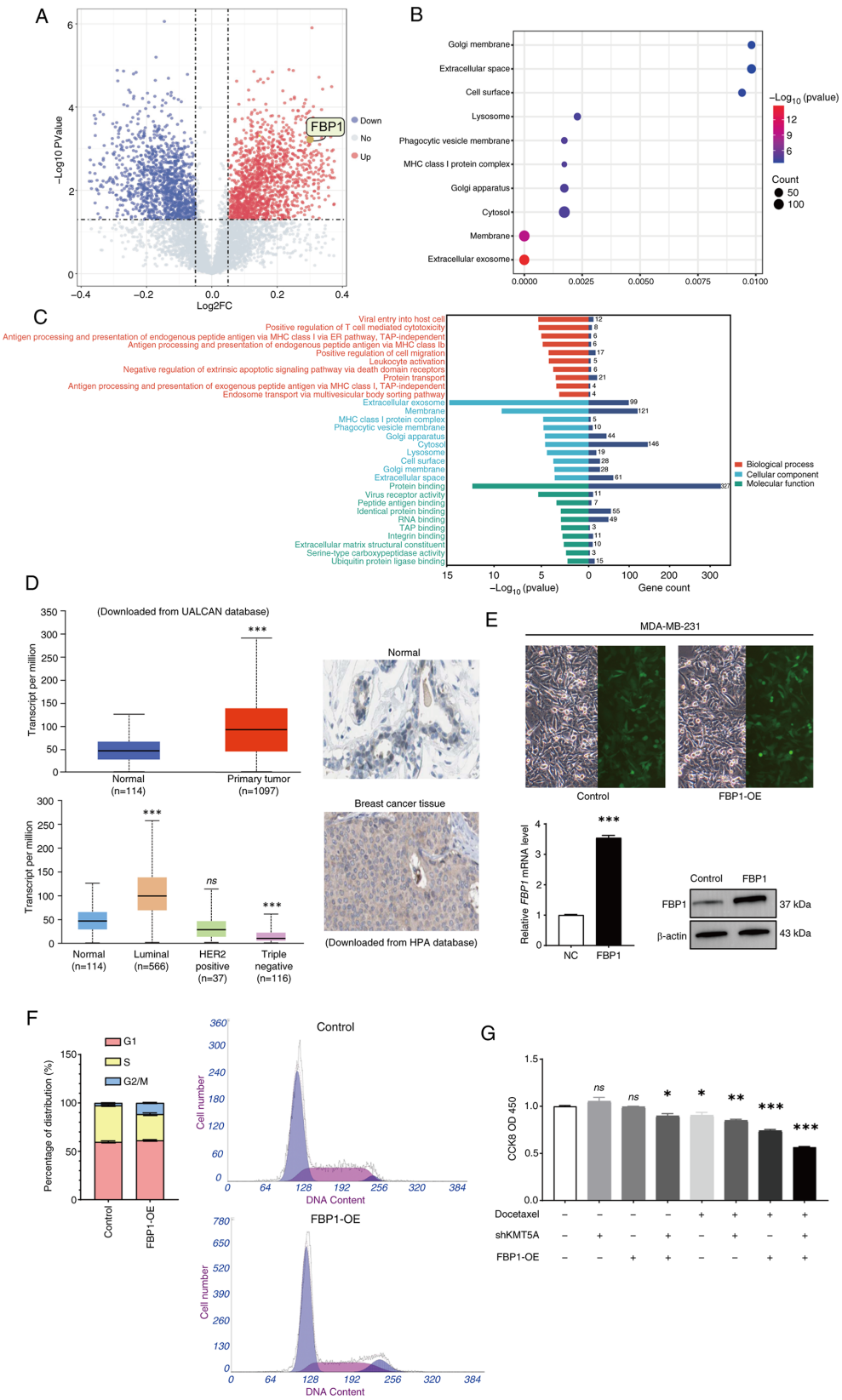

Figure 2. FBP1 is upregulated by KMT5A knockdown. (A) Volcano map demonstrating 414 differentially expressed proteins between control (n=3) and KMT5A-knockdown groups (n=3). Red indicates upregulation, and blue indicates deregulation. (B) Kyoto Encyclopedia of Genes and Genomes pathway enrichment analysis of 414 target proteins. (C) GO analysis of 414 target proteins. The colors represent GO functional categories (red: Biological Process, green: Molecular Function, blue: Cellular Component). The length of the bar chart to the right of the origin indicates the number of different expressed proteins included in the function. (D) Expression of FBP1 in breast cancer. (E) After 72 h of infection, cells were observed and images were captured by fluorescence microscope. Magnification, x100. Expression of FBP1 in breast cancer cells was detected by reverse transcription-quantitative PCR and western blotting. (F) The cell cycle analysis of the FBP1-overexpressing group. (G) CCK-8 assay was used to detect the cell viability and proliferation after the addition of docetaxel. *P<0.05, **P<0.01 and ***P<0.001. FBP1, fructose-1,6-bisphosphatase; KMT5A, lysine methyltransferase 5A; GO, Gene Ontology; CCK-8, Cell Counting Kit-8; DTX, docetaxel; UALCAN, the university of Alabama at Birmingham database; HPA, human protein atlas; sh-, short hairpin; NC, negative controls; OE, overexpression; ns, no significance (P≥0.05).

of FBP1was significantly increased in BRCA, however there were significant differences among the different subtypes. FBP1 was significantly increased in luminal BRCA (P<0.05) but significantly decreased in triple-negative BRCA (P<0.05) (Fig. 2D). IHC also demonstrated that FBP1 was highly expressed in BRCA tissues (Fig. 2D). Inadequately, IHC cannot divide into different subtypes. IHC results of FBP1 in BRCA and adjacent normal breast tissue were obtained from the HPA database and could not be differentiated into different subtypes for analysis.

MDA-MB-231 cells were transfected with the lentivirus LVCON238 (negative control) or LVKL68505-2 (FBP1-OE). RT-qPCR also revealed that the mRNA level of FBP1 was significantly increased in cells transfected with the lentivirus LVKL68505-2 (FBP1-OE) (P<0.05) (Fig. 2E). Western blot analysis revealed that FBP1 was markedly overexpressed in MDA-MB-231 cells transfected with the lentivirus LVKL68505-2 (FBP1-OE) (Fig. 2E).

Effect of FBP1 on the cell cycle and chemotherapy resistance. After overexpression of FBP1, the proportion of G2/M phase cells increased significantly (Fig. 2F). DTX is a G2/M phase cycle-specific drug, and overexpression of FBP1 may enhance the proapoptotic effect of DTX on BRCA cells. Therefore, the effect of overexpression of FBP1 was detected on cell proliferation using a CCK-8 assay and MDA-MB-231 cells were subsequently treated with DTX. After the addition of the DTX (20 μM), cell proliferation was further inhibited in the FBP1 overexpression group (Fig. 2G).

FBP1 is downregulated by KMT5A overexpression. TCGA-BRCA data were downloaded from the TCGA database. The expression of FBP1 was negatively correlated with that of KMT5A [Pearson correlation coefficient (r=-0.131, P<0.05] (Fig. 3A). To verify the relationship between KMT5A and FBP1, the expression of FBP1 was detected after knocking down KMT5A in MDA-MB-231 cell line. The expression of FBP1 was increased in the shKMT5A group (Fig. 3B). A dual-luciferase reporter gene assay was used to determine the regulatory relationship between KMT5A and FBP1. The NC-Luc + KMT5A-WT group and the FBP1-Promoter-Luc + vector group were designed to observe the internal interaction between the reporter vector and the internal reference vector to eliminate the background influence. The luciferase activity of the FBP1-Promoter-Luc + KMT5A-WT group was lower than that of the FBP1-Promoter-Luc+vector group and NC-Luc + KMT5A-WT group. The results revealed that FBP1 demonstrated strong promoter activity when KMT5A was not expressed. Thus, it was found that KMT5A inhibits FBP1 after the exclusion of endogenous influences (Fig. 3C).

FBP1 overexpression combined with KMT5A knockdown inhibits MDA-MB-231 cell line proliferation. To determine whether FBP1 has a reverse regulatory effect on KMT5A, a lentivirus was used to construct a NC group, an FBP1 overexpression group (FBP1-OE), a KMT5A low-expression group (shKMT5A) and an FBP1 overexpression + KMT5A low-expression group (FBP1-OE + shKMT5A). Moreover, RT-qPCR and western blot analysis successfully verified that FBP1 was overexpressed and KMT5A was downregulated in the MDA-MB-231 cell line (Fig. 3D).

When DTX was not added, no matter whether KMT5A was knocked down alone (shKMT5A) or FBP1 was overexpressed (FBP1-OE), the proliferation inhibition rate of MDA-MB-231 cells was not significantly different from that of the NC group. However, the inhibitory rate of cell proliferation in the FBP1-OE + shKMT5A group was 10.3±4.4%. After addition of DTX, the cell proliferation inhibition rate was 26.1±2.6% in the FBP1-OE group alone, 15.2±2.7% in the shKMT5A group alone, however increased to 43.4±1.3% in the FBP1-OE + shKMT5A group. Neither the overexpression of FBP1 nor low expression of KMT5A alone affected the proliferation of BRCA cells. When KMT5A was simultaneously expressed at low levels and FBP1 was overexpressed, the proliferation of BRCA cells was significantly inhibited after DTX (20 μM) was added (Fig. 2G). It was also revealed that the MDA-MB-231 cell activity decreased to ~55.8 and 41.0% respectively after DTX addition without/with FBP1 overexpression. As demonstrated in Fig. 2G, the MDA-MB-231 cell activity decreased to ~91.4 and 73.9% respectively after DTX addition without/with FBP1 overexpression. Therefore, after the addition of DTX, overexpression of FBP1 or/and downregulation of KMT5A jointly inhibited the proliferation of MDA-MB-231 cells.

The effect of KMT5A on chemotherapeutic drug resistance and glycolysis depends on methylase activity. UNC0379 is a selective inhibitor of KMT5A, however it can also target other histone methyltransferases apart from KMT5A (28). The DTX groups contain both DTX (20 μM) and DTX solvent. UNC0379 (0, 5 or 10 μM) was added respectively the DTX solvent groups and DTX groups. As it can be observed, UNC0379 can also cooperate with DTX to inhibit the proliferation of BRCA cells. Moreover, the change in concentration of UNC0379 can enhance the inhibitory effect on the proliferation of BRCA cells. As the concentration UNC0379 was increased, MDA-MB-231 cell proliferation was more strongly inhibited (Fig. 4A).

As the concentration of the inhibitor UNC0379 increased, the amount of lactic acid produced by the BRCA cells decreased (Fig. 4B). Moreover, after the addition of the inhibitor UNC0379, the glucose uptake of BRCA cells was also significantly reduced (Fig. 4C).

KMT5A inhibits FBP1 expression through methylase activity. As revealed in Fig. 3C, FBP1 promoter activity decreased when KMT5A-WT was overexpressed. To further verify whether KMT5A methylase activity affects FBP1 transcription, a KMT5A mutant (KMT5A-R295G) was added to the FBP1 promoter. Both KMT5A-WT and KMT5A-R295G inhibited FBP1 gene expression. Therefore, compared with the NC-Luc + Vector (control) group, the relative activity of luciferase in both groups decreased. The results also revealed that when KMT5A lost methylase activity, FBP1 promoter activity increased compared with KMT5A-WT group (Fig. 4D). This suggests that KMT5A has an inhibitory effect on the activation and regulation of FBP1 promoter depending on its methylase activity.

How does KMT5A affect FBP1 expression through methylase activity? Yang *et al* (29) demonstrated that SET8

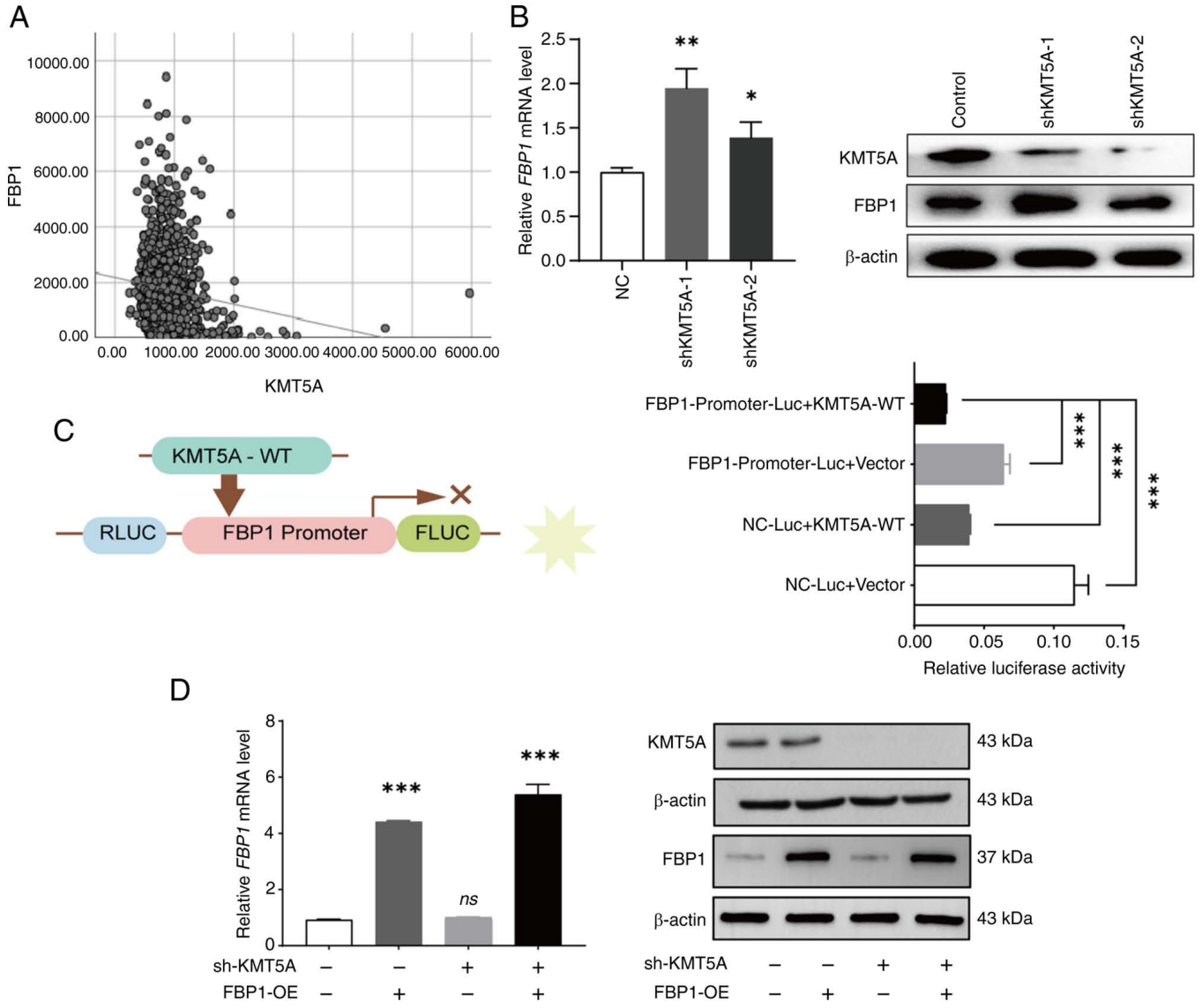

Figure 3. KMT5A inhibits FBP1 expression. (A) Correlation between the expression of KMT5A and FBP1 based on TCGA cohort [Pearson correlation coefficient (r)=0.131, P<0.05]. (B) The expression of FBP1 was detected by RT-qPCR and western blotting after KMT5A was knocked down. (C) The relationship between KMT5A and FBP1 was verified by dual-luciferase reporter gene assay. (D) The effect of infection of shKMT5A and FBP1 lentivirus in the breast cancer cells were detected by RT-qPCR and western blotting. *P<0.05, **P<0.01 and ***P<0.001. KMT5A, lysine methyltransferase 5A; FBP1, fructose-1,6-bisphosphatase; RT-qPCR, reverse transcription-quantitative PCR; sh-, short hairpin; NC, negative controls; WT, wild-type; RLUC, *Renilla* luciferase; FLUC, firefly luciferase; Luc, luciferase; OE, overexpression; ns, no significance (P≥0.05).

and TWIST commonly promote epithelial-mesenchymal transformation and enhance the invasive potential of BRCA cells. In BRCA, KMT5A (SETD8) interacts with TWIST and synergistically upregulates N-Cadherin and downregulates E-Cadherin at the transcriptional level. The HPA database was utilized to search for an interaction network between KMT5A and TWIST and discovered that there was indeed an interaction between the two (Fig. 4E). Based on the prediction of binding sites between FBP1 promoter and TWIST1, dual-luciferase reporter gene experiment was used to verify whether TWIST1 had an effect on promoter activation and regulation. Using empty plasmids as controls, results revealed that overexpression of TWIST1 can increase FBP1 promoter activity by ~5-fold, suggesting that TWIST1 activates FBP1 promoter activity (Fig. 4F).

Discussion

Primary or acquired resistance to chemotherapy is a major barrier to BRCA treatment. The main reasons for chemotherapy failure include: i) Inadequate pharmacokinetic properties of the drug (30); ii) tumor cell-intrinsic factors, such as the expression of drug efflux pumps, altered cellular homeostasis, and glucose metabolism; and iii) the tumor microenvironment, characterized by hypoxia and acidosis (31). The mechanism of DTX resistance in BRCA is multifaceted. The present study focused on drug resistance induced by changes in glucose metabolism, and targeting glycolytic enzyme activities could be a useful strategy for cancer therapy (32).

In the present study, it was revealed that KMT5A was highly expressed in DTX-resistant BRCA cells. Analysis of protein expression differences after KMT5A knockdown revealed

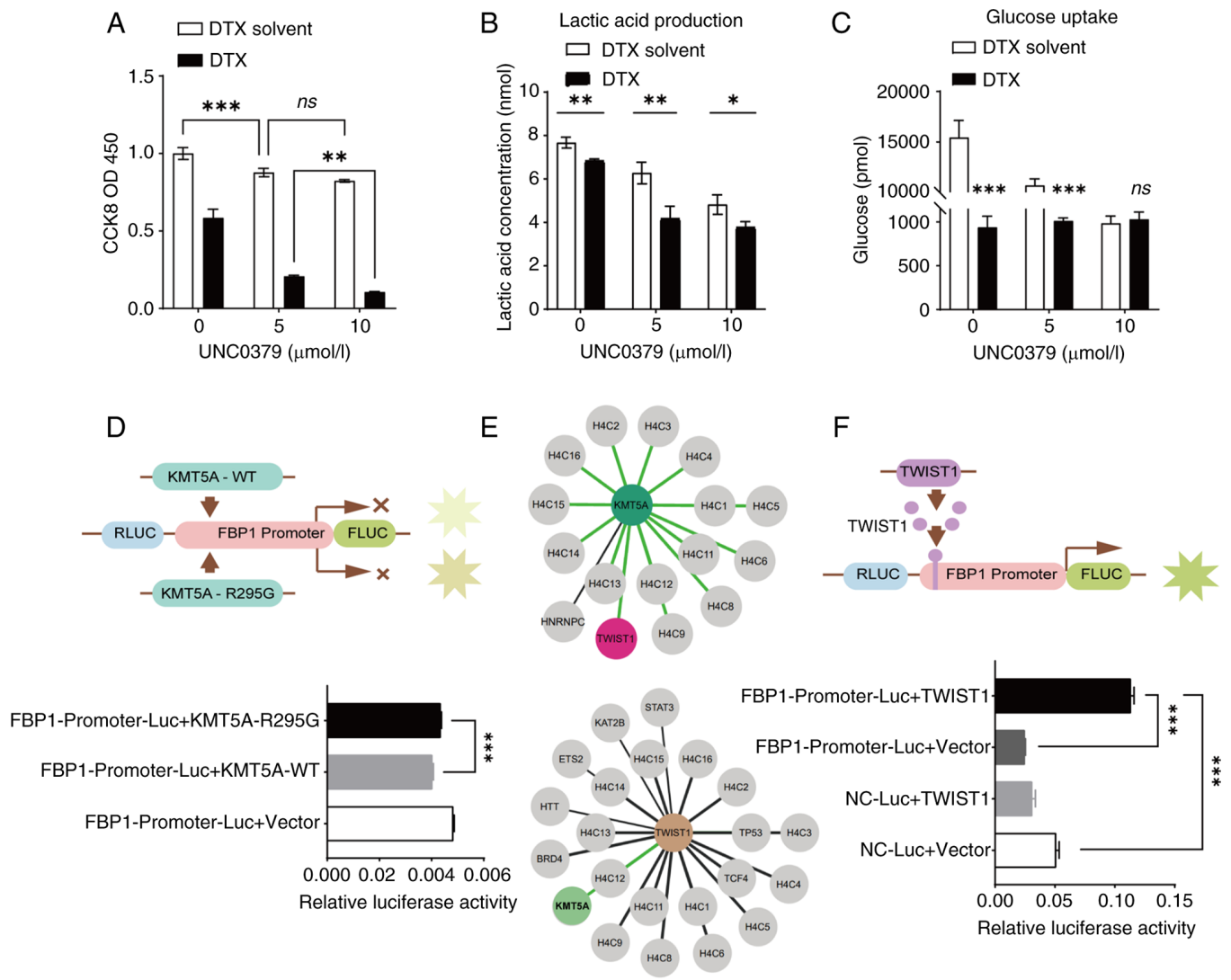

Figure 4. KMT5A relies on methylase activity to inhibit FBP1. (A) KMT5A inhibitor UNC0379 was used to treat breast cancer cells to detect cell activity. (B and C) MDA-MB-231 cells were treated with KMT5A inhibitor UNC0379 to detect lactic acid production and glucose uptake. (D) The effect of KMT5A methylation activity on the FBP1 promoter was detected by dual-luciferase reporter gene assay. KMT5A-R295G is a mutant without methylase activity. (E) The Human Protein Atlas database (https://www.proteinatlas.org/) revealed the interaction networks of KMT5A and TWIST1. (F) Correlation between TWIST1 and FBP1 promoter was detected by dual-luciferase reporter gene assay. ns, $P \geq 0.05$; $^{*}P<0.05$, $^{**}P<0.01$ and $^{***}P<0.001$. KMT5A, lysine methyltransferase 5A; FBP1, fructose-1,6-bisphosphatase; TWIST1, twist family BHLH transcription factor 1; DTX, docetaxel; WT, wild-type; RLUC, *Renilla* luciferase; FLUC, firefly luciferase; Luc, luciferase; ns, no significance ($P \geq 0.05$).

significant changes in signalling pathways related to glucose metabolism. FBP1, a key gluconeogenic enzyme, was significantly upregulated. Dual-luciferase reporter assays confirmed that KMT5A inhibited the expression of FBP1, and glucose uptake and lactic acid production experiments revealed that KMT5A inhibited gluconeogenesis and promoted anaerobic glycolysis of glucose. Because KMT5A inhibits the transcription factor TWIST1, it was verified that TWIST1 promotes the expression of FBP1 through a dual-luciferase reporter assay. Therefore, KMT5A reduces the ratio of G2/M phase cells and reduces the sensitivity of cells to DTX by decreasing the ability of TWIST1 to promote FBP1 expression. Conversely, after the upregulation of FBP1 and the downregulation of KMT5A, the sensitivity of MDA-MB-231 cells to DTX increased. Due to the lack of experiments to directly verify the interaction between KMT5A and TWIST1, the correlation between the two genes via several websites were analysed and it was deduced that KMT5A indirectly affects TWIST1. Moreover, Yang *et al* (29) revealed that KMT5A confers dual transcriptional activity on TWIST1 in BRCA, which also confirms this point.

A previous study by the authors demonstrated a positive correlation between KMT5A and HIF1α and HIF1α target genes and validated KMT5A as a novel metabolic reprogramming regulator (20) (Fig. 5). Ectopic expression of miR-335 or depletion of its target gene KMT5A can enhance the sensitivity of paclitaxel-resistant BRCA cells to paclitaxel (32). Additionally, overexpression of KMT5A induces DTX chemoresistance in BRCA. However, the possible mechanism through which KMT5A promotes chemotherapy resistance in BRCA through regulating glucose metabolism has not been reported, and the present study research shed additional light on this topic.

Some limitations should also be considered and discussed when interpreting these results and presenting

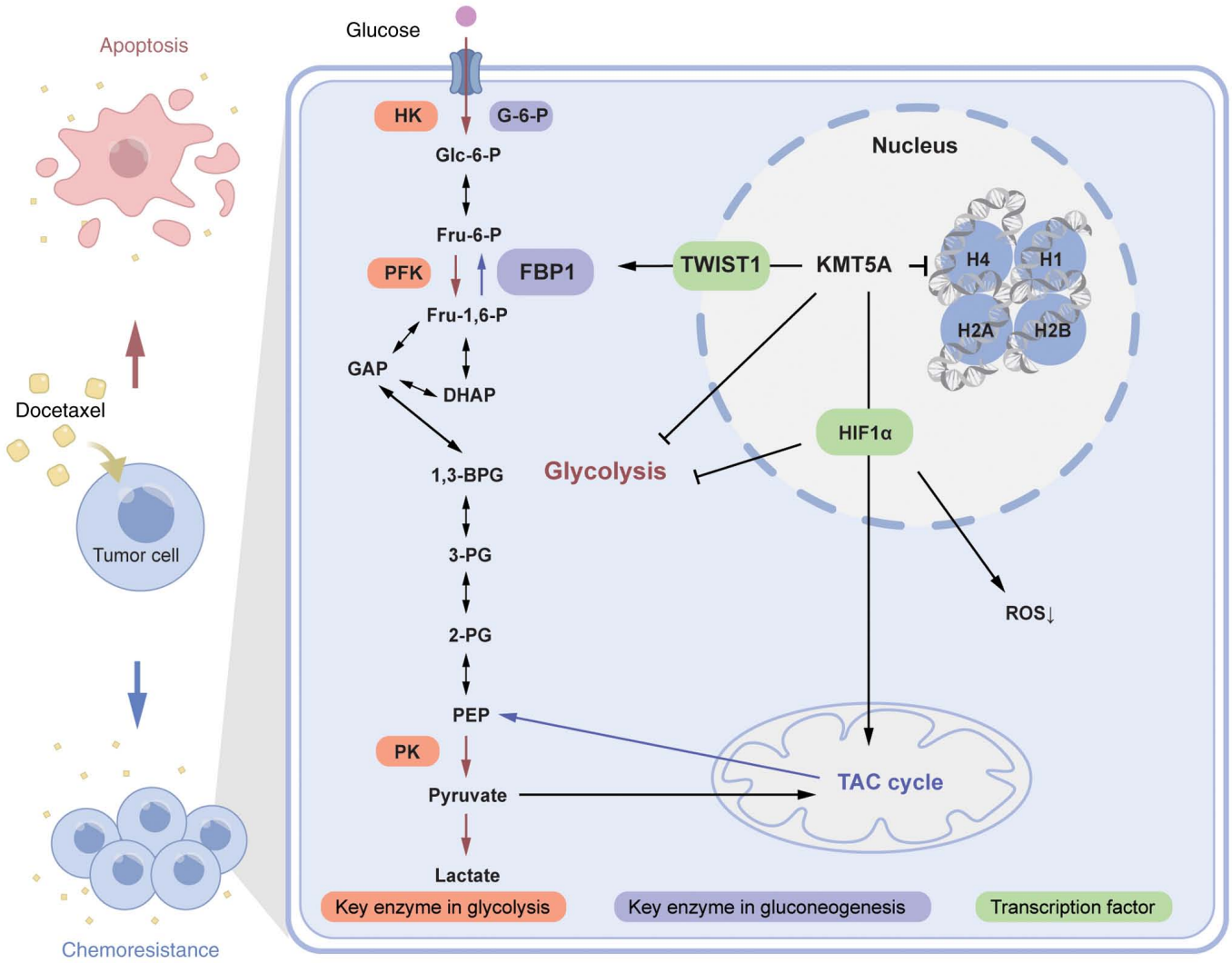

Figure 5. The mechanism by which KMT5A inhibits FBP1 and thus promotes docetaxel resistance in breast cancer. KMT5A, lysine methyltransferase 5A; FBP1, fructose-1,6-bisphosphatase; TWIST1, twist family BHLH transcription factor 1.

their contributions. First, on account of cumulative evidence, It was concluded that KMT5A plays an important role in BRCA development by inducing cancer cell multiplication and chemotherapy resistance. However, additional functional experiments are needed to further explore the complex underlying mechanisms *in vitro* and *in vivo*. Due to the small sample size of the present study's trial, the expression level of KMT5A in different subtypes of BRCA was revealed through the UALCAN database and the IHC of different subtypes of BRCA was not discussed. While KMT5A may decrease the sensitivity of BRCA to DTX, it may also promote the metastasis of some types of BRCA. For example, Yu *et al* (33) discovered that KMT5A expression is significantly associated with activated Hippo/YAP signaling and promoted triple-negative BRCA metastasis. Moreover, due to the relatively small sample size of the survival and KMT5A expression analyses, replication studies in larger populations and more ethnicities are needed to validate these results.

In conclusion, the findings of the present study confirmed that KMT5A induces DTX resistance in BRCA by affecting glucose metabolism and that the knockdown or inhibition of KMT5A expression may reverse chemotherapy resistance in patients and improve the prognosis of patients with BRCA. Future studies should focus on investigating the detailed mechanisms by which KMT5A regulates the activity of other metabolic pathways and its possible regulatory role in other tumors.

Acknowledgements

Not applicable.

Funding

The present study was supported by the National Science Foundation of China (grant no. 8177101282).

Availability of data and materials

The data generated in the present study may be requested from the corresponding author. The data generated in the present study may be found in the iProX database under accession number IPX0008291000 or at the following URL: https://www.iprox.cn//page/SCV017.html?query=IPX0008291000.

Authors' contributions

XP, LM, XC, FT and XZ made substantial contributions to the conception. XZ made substantial contributions to the study design. XP and LM participated in the laboratory work and data analyses. XP and XZ confirm the authenticity of all the raw data. All authors participated in drafting or revising the content for important intellectual content, and read and approved the final manuscript.

Ethics approval and consent to participate

The present study was approved (approval no. YS-2017-006) by the ethics committee of Shanghai Sixth Peoples Hospital Affiliated to Shanghai Jiao Tong University School of Medicine (Shanghai, China). Written informed consent was obtained from all the participants before the enrolment and publication of the present study. The present study was certifiably performed following the 1964 declaration of HELSINKI and later amendments.

Patient consent for publication

Not applicable.

Competing interests

The authors declare that they have no competing interests.

Use of artificial intelligence tools

During the preparation of this work, artificial intelligence tools were used to improve the readability and language of the manuscript, and subsequently, the authors revised and edited the content produced by the artificial intelligence tools as necessary, taking full responsibility for the ultimate content of the present manuscript.

References

1. Miller KD, Nogueira L, Devasia T, Mariotto AB, Yabroff KR, Jemal A, Kramer J and Siegel RL: Cancer treatment and survivorship statistics, 2022. CA Cancer J Clin 72: 409-436, 2022.
2. Fan L, Strasser-Weippl K, Li JJ, St Louis J, Finkelstein DM, Yu KD, Chen WQ, Shao ZM and Goss PE: Breast cancer in China. Lancet Oncol 15: E279-E289, 2014.
3. Vasan N, Baselga J and Hyman DM: A view on drug resistance in cancer. Nature 575: 299-309, 2019.
4. Chen H, Zhang M and Deng Y: Long noncoding RNAs in Taxane resistance of breast cancer. Int J Mol Sci 24: 12253, 2023.
5. Sajid A, Rahman H and Ambudkar SV: Advances in the structure, mechanism, and targeting of chemoresistance-linked ABC transporters. Nat Rev Cancer 23: 762-779, 2023.
6. Cao X, Hou J, An Q, Assaraf YG and Wang X: Towards the overcoming of anticancer drug resistance mediated by p53 mutations. Drug Resist Updat 49: 100671, 2020.
7. Di Pietro A, Dayan G, Conseil G, Steinfels E, Krell T, Trompier D, Baubichon-Cortay H and Jault J: P-glycoprotein-mediated resistance to chemotherapy in cancer cells: Using recombinant cytosolic domains to establish structure-function relationships. Braz J Med Biol Res 32: 925-939, 1999.
8. Bukowski K, Kciuk M and Kontek R: Mechanisms of multidrug resistance in cancer chemotherapy. Int J Mol Sci 21: 3233, 2020.
9. Dominiak A, Chełstowska B, Olejarz W and Nowicka G: Communication in the cancer microenvironment as a target for therapeutic interventions. Cancers (Basel) 12: 1232, 2020.
10. Bishayee K, Lee SH and Park YS: The Illustration of altered glucose dependency in drug-resistant cancer cells. Int J Mol Sci 24: 13928, 2023.
11. Xu L, Zhang L, Sun J, Hu X, Kalvakolanu DV, Ren H and Guo B: Roles for the methyltransferase SETD8 in DNA damage repair. Clin Epigenetics 14: 34, 2022.
12. Al Temimi AHK, Martin M, Meng Q, Lenstra DC, Qian P, Guo H, Weinhold E and Mecinović J: Lysine Ethylation by histone lysine methyltransferases. Chembiochem 21: 392-400, 2020.
13. Kukita A, Sone K, Kaneko S, Kawakami E, Oki S, Kojima M, Wada M, Toyohara Y, Takahashi Y, Inoue F, *et al*: The Histone Methyltransferase SETD8 regulates the expression of tumor suppressor genes via H4K20 methylation and the p53 signalling pathway in endometrial cancer cells. Cancers (Basel) 14: 5367, 2022.
14. Wada M, Kukita A, Sone K, Hamamoto R, Kaneko S, Komatsu M, Takahashi Y, Inoue F, Kojima M, Honjoh H, *et al*: Epigenetic modifier SETD8 as a therapeutic target for high-grade serous ovarian cancer. Biomolecules 10: 1686, 2020.
15. Liao T, Wang YJ, Hu JQ, Wang Y, Han LT, Ma B, Shi RL, Qu N, Wei WJ, Guan Q, *et al*: Histone methyltransferase KMT5A gene modulates oncogenesis and lipid metabolism of papillary thyroid cancer *in vitro*. Oncol Rep 39: 2185-2192, 2018.
16. Herviou L, Ovejero S, Izard F, Karmous-Gadacha O, Gourzones C, Bellanger C, De Smedt E, Ma A, Vincent L, Cartron G, *et al*: Targeting the methyltransferase SETD8 impairs tumor cell survival and overcomes drug resistance independently of p53 status in multiple myeloma. Clin Epigenetics 13: 174, 2021.
17. Li B, Qiu B, Lee DS, Walton ZE, Ochocki JD, Mathew LK, Mancuso A, Gade TP, Keith B, Nissim I and Simon MC: Fructose-1,6-bisphosphatase opposes renal carcinoma progression. Nature 513: 251-255, 2014.
18. Li H, Li M, Pang Y, Liu F, Sheng D and Cheng X: Fructose-1,6-bisphosphatase-1 decrease may promote carcinogenesis and chemoresistance in cervical cancer. Mol Med Rep 16: 8563-8571, 2017.
19. Li H, Qi Z, Niu Y, Yang Y, Li M, Pang Y, Liu M, Cheng X, Xu M and Wang Z: FBP1 regulates proliferation, metastasis, and chemoresistance by participating in C-MYC/STAT3 signalling axis in ovarian cancer. Oncogene 40: 5938-5949, 2021.
20. Huang R, Yu Y, Zong X, Li X, Ma L and Zheng Q: Monomethyltransferase SETD8 regulates breast cancer metabolism via stabilizing hypoxia-inducible factor 1α. Cancer Lett 390: 1-10, 2017.
21. Livak KJ and Schmittgen TD: Analysis of relative gene expression data using real-time quantitative PCR and the 2(-Delta Delta C(T)) method. Methods 25: 402-408, 2001.
22. Thul PJ and Lindskog C: The human protein atlas: A spatial map of the human proteome. Protein Sci 27: 233-244, 2018.
23. Chandrashekar DS, Bashel B, Balasubramanya SAH, Creighton CJ, Ponce-Rodriguez I, Chakravarthi BVSK and Varambally S: UALCAN: A portal for facilitating tumor subgroup gene expression and survival analyses. Neoplasia 19: 649-658, 2017.
24. Ghandi M, Huang FW, Jané-Valbuena J, Kryukov GV, Lo CC, McDonald ER III, Barretina J, Gelfand ET, Bielski CM, Li H, *et al*: Next-generation characterization of the cancer cell line encyclopedia. Nature 569: 503-508, 2019.
25. Kenicer J, Spears M, Lyttle N, Taylor KJ, Liao L, Cunningham CA, Lambros M, MacKay A, Yao C, Reis-Filho J and Bartlett JM: Molecular characterisation of isogenic taxane resistant cell lines identify novel drivers of drug resistance. BMC Cancer 14: 762, 2014.
26. Jørgensen S, Elvers I, Trelle MB, Menzel T, Eskildsen M, Jensen ON, Helleday T, Helin K and Sørensen CS: The histone methyltransferase SET8 is required for S-phase progression. J Cell Biol 179: 1337-1345, 2007.
27. Sousa-Pimenta M, Estevinho LM, Szopa A, Basit M, Khan K, Armaghan M, Ibrayeva M, Sönmez Gürer E, Calina D, Hano C and Sharifi-Rad J: Chemotherapeutic properties and side-effects associated with the clinical practice of terpene alkaloids: Paclitaxel, docetaxel, and cabazitaxel. Front Pharmacol 14: 1157306, 2023.
28. Ma A, Yu W, Li F, Bleich RM, Herold JM, Butler KV, Norris JL, Korboukh V, Tripathy A, Janzen WP, *et al*: Discovery of a selective, substrate-competitive inhibitor of the lysine methyltransferase SETD8. J Med Chem 57: 6822-6833, 2014.
29. Yang F, Sun L, Li Q, Han X, Lei L, Zhang H and Shang Y: SET8 promotes epithelial-mesenchymal transition and confers TWIST dual transcriptional activities. EMBO J 31: 110-123, 2012.

30. Wang X, Cao C, Tan X, Liao X, Du X, Wang X, Liu T, Gong D, Hu Z and Tian X: SETD8, a frequently mutated gene in cervical cancer, enhances cisplatin sensitivity by impairing DNA repair. Cell Biosci 13: 107, 2023.
31. Phan LM, Yeung SC and Lee MH: Cancer metabolic reprogramming: Importance, main features, and potentials for precise targeted anticanceranti-cancer therapies. Cancer Biol Med 11: 1-19, 2014.
32. Wang Y, Wang H, Ding Y, Li Y, Chen S, Zhang L, Wu H, Zhou J, Duan K, Wang W, *et al*: N-peptide of vMIP-II reverses paclitaxel-resistance by regulating miRNA-335 in breast cancer. Int J Oncol 51: 918-930, 2017.
33. Yu B, Su J, Shi Q, Liu Q, Ma J, Ru G, Zhang L, Zhang J, Hu X and Tang J: KMT5A-methylated SNIP1 promotes triple-negative breast cancer metastasis by activating YAP signaling. Nature Commun 13: 2192, 2022.